Research Square

Preprints are preliminary reports that have not undergone peer review.
They should not be considered conclusive, used to inform clinical practice,
or referenced by the media as validated information.

The COOLCITY Index: Climate Adaptation Potential Assessment of Blue-Green Infrastructure in 11,041 European Union Cities Using Remote Sensing

Dominik Kopeć

dominik.kopec@biol.uni.lodz.pl

Uniwersytet Lodzki https://orcid.org/0000-0003-0831-2992

Agata Tarkowska

MGGP Aero

Martyna Wietecha

Uniwersytet Łódzki: Uniwersytet Lodzki

Jan Jedliński

MGGP AERO

Dominik Żmuda

MGGP Aero

Aram Takmadżan

MGGP Aero

Aleksandra Krzywicka

MGGP Aero

Alicja Śniadach

Uniwersytet Gdański: Uniwersytet Gdanski

Robert Migas

MGGP Aero

Zuzanna Kunert

MGGP Aero

Jakub Charyton

MGGP Aero

Łukasz Sławik

MGGP Aero

Research Article

Keywords:

Posted Date: June 16th, 2026

DOI: https://doi.org/10.21203/rs.3.rs-9817347/v1

License: This work is licensed under a Creative Commons Attribution 4.0 International License.
Read Full License

Abstract

Progressive climate change is amplifying environmental pressure on European cities. In the face of growing threats such as water stress and the degradation of urban green spaces, the capacity of cities to adapt to climate change has become a key concern. The aim of this study is to assess the adaptive potential of 11,041 of the largest cities across the European Union in relation to the condition of their environmental resources. The analysis is based on data from 2025 and uses the COOLCITY Index. The remote sensing data was acquired from publicly available satellite missions and used to generate a set of raster maps further calculated into spatial and integrated indicators. The integrated indicators were then aggregated into the COOLCITY Index enabling comparative analyses across cities and countries. The results indicate that COOLCITY Index shows substantial spatial heterogeneity across cities in the European Union. Pronounced differences are observed between countries. An analysis of national averages shows that the lowest COOLCITY Index is recorded in Cyprus (2.1), while the highest is observed in Finland (7.1), highlighting the extent of variation among member states. COOLCITY Index is strongly related to latitude ($\beta = +0.519$) and population density ($\beta = -0.408$), indicating that cities in cooler, and less densely populated areas generally exhibit higher adaptive potential of blue-green infrastructure. The proposed approach enables systematic long-term monitoring and provides a practical tool to support adaptation policies and the implementation of nature-based solutions.

1. Introduction

1.1. Urban Resilience to Climate Change in Europe: The Role of Blue-Green Infrastructure

Climate change is one of the foremost environmental challenges facing Europe. Over recent decades, trends such as rising average air temperatures, shifts in precipitation patterns, increasing frequency and intensity of extreme events, like prolonged periods of drought and heatwaves have been observed (IPCC 2021; IPCC 2022). Climate projections indicate that these processes are expected to intensify further in the coming decades placing growing pressure on urban areas (IPCC 2021). Therefore, because 72–79% of the European Union (EU) population lives in urban areas, this issue is of critical importance. (Dematteis 2029). The impacts of climate change in Europe are also characterized by pronounced regional variability. In southern Europe, increasing water stress represents the primary challenge (European Environment Agency 2024), while in northern regions, rising temperatures and threats to biodiversity - including disruptions to ecosystem functioning - are of great concern (European Environment Agency 2025). The urban heat island effect, driven by impervious surfaces and limited vegetation cover, results in substantially higher temperatures compared with surrounding rural areas. Surface sealing and insufficient stormwater retention exacerbate urban vulnerability to heavy rainfall and localized flooding, while also amplifying water deficits during dry periods (European Environment Agency 2025).

Building a city's adaptive potential requires a systemic approach that takes climate-related hazards into account. A well-adapted city does not only minimize the negative impacts of extreme weather events but also actively strengthens its long-term adaptive capacity through planning, implementation of actions, and continuous monitoring of their effectiveness. These concepts are defined as urban resilience and adaptation to climate change (IPCC 2022). Adaptation is a continuous process encompassing both preparedness and response to the climate change impacts (European Environment Agency 2024). A key element enhancing urban resilience is blue-green infrastructure (BGI; European Commission 2019; Almaaitah et al. 2021). It comprises networks of urban greenery, parks, ecological corridors, stormwater retention systems, natural ponds and river channels. Numerous studies show that BGI effectively mitigates urban heat islands (Balany et al 2020; Kumar et al 2024), improves stormwater retention (Dobkowitz et al. 2025) and reduces flood risk (Ferreira et al. 2024). The effectiveness of BGI results both from its regulatory functions and from its potential to be integrated into urban spaces, aligning ecological goals with social objectives.

Urban climate adaptation measures are embedded within the broader framework of European Union (EU) policy, including the European Green Deal, the Smart Cities initiative, and the EU Strategy on Adaptation to Climate Change (European Commission 2021). EU policy emphasizes the importance of proactive measures, the integration of nature-based solutions (NBS) into urban planning, and the use of monitoring data to evaluate the effectiveness of implemented actions. This approach is particularly relevant given the increasing climate risks faced by European cities and enables the alignment of local actions with national and EU-level climate policy objectives through the implementation of BGI (European Commission 2019).

1.2. Monitoring Urban Adaptive Potential

Remote sensing and geographic information systems represent widely applied methodologies in environmental monitoring and spatial analysis and are extensively documented as addressing urban climate, ecosystem services, and climate change adaptation issues (Di Palma et al. 2024; Araya-Muñoz et al. 2016). Satellite-based observations are especially valuable in this regard, as they ensure methodological objectivity and long-term temporal consistency essential for monitoring environmental changes and assessing adaptation processes in cities (Farooq et al 2024). The most commonly used satellite missions in urban environmental research include the Landsat programme (Landsat 5, 7, 8, and 9), the Sentinel-2 mission within the Copernicus programme and MODIS products for large-scale or long-term analyses (Moreno et al. 2023). These missions differ in spatial, temporal, and spectral resolution, which determines their suitability for specific research objectives. Several satellite-derived products and indices have emerged as standard tools for assessing environmental conditions in cities. Among the most frequently applied are vegetation indices, particularly the Normalized Difference Vegetation Index (NDVI), which serves as a proxy for vegetation presence, density, and condition (Chahbi et al. 2025; Martins et al. 2025). Thermal indicators, especially Land Surface Temperature (LST) derived from thermal infrared bands of Landsat sensors, are commonly used to analyse urban heat patterns (Wagner et al. 2023) and the urban surface heat island effect (Dimitrov et al. 2024). Although numerous studies

have demonstrated the use of remote sensing in environmental research, most existing studies remain limited in scope, focusing on single cities (Falda et al. 2025). Moreover, many analyses address only one adaptation aspect at a time, such as heat mitigation (Sola-Caraballo et al. 2025) or changes in vegetation cover (di Cristofaro et al. 2022). It is also important to acknowledge the role of the Copernicus Land Monitoring Service (CLMS), which provides harmonized, pan-European geospatial datasets on land cover, land use, vegetation, and biophysical parameters (Copernicus Land Monitoring Service 2026). However, a key limitation of CLMS products is their temporal resolution and update frequency. Many datasets are not updated annually, which may reduce their applicability for near-real-time monitoring or analyses of rapidly changing urban processes.

Integrated indicators are designed to transform multiple variables into comparable values that can be easily interpreted by both decision-makers and city residents (Psatha 2025). Methodologically, their construction involves selecting partial indicators that represent the studied aspects, normalizing them to a common scale, and aggregating them into a single composite index (Nardo 2005; Saisana and Saltelli 2011). Such an index may, for example, provide a synthetic assessment of the adaptive potential of cities. Composite indices have become an effective and widely used tool for supporting policymakers in decision-making and for raising public awareness of environmental challenges (Mackres et al. 2023). Their application is multidimensional and covers various stakeholder groups, in particular, they can support public policy by monitoring progress in implementing key strategies, such as the EU Strategy on Adaptation to Climate Change (EU Commission 2013). At the city level, these indices also enable benchmarking of cities, which supports: (a) the assessment of the condition of BGI, b) the exchange of experience and best practices of implementing BGI between comparable cities. Such integrated indicators can also support the building of urban partnerships within projects aimed at enhancing climate resilience (Tyler et al. 2016).

Examples of existing integrated indicators demonstrate a variety of methodological approaches and thematic scopes, reflecting different research and application objectives. Nedkov et al. (2017) developed an integrated index that focuses on assessing the condition of urban ecosystems and the services they provide, integrating spatial and functional data. Deslauriers et al. (2018) developed the City Biodiversity Index related to the connectivity of natural areas in cities, emphasizing the importance of ecological continuity as a key element in assessing urban biodiversity. This approach is more specialized and focuses on a single aspect of urban system functioning. In turn, Ferreira et al. (2024), propose a BGI effectiveness indicator in the context of integrated urban water management, which combines hydrological, environmental, and infrastructural components, enabling the assessment of the effectiveness of BGI solutions in adapting to climate change.

The aim of this study is to assess the adaptive potential of 11,041 EU cities according to their environmental conditions in relation to five spatial aspects — water conditions, surface permeability, vegetation diversity, vegetation state, and thermal conditions — integrated into the COOLCITY Index (CCI). Why 11,041 cities? This number covers almost all urban areas in the studied countries, giving the research a unique scale and practical value. This allows CCI to include smaller administrative units,

which are often overlooked in support towards adaptive decision-making. The study addresses the following research questions:

1. Which variables characterising European Union cities are correlated with the state of blue-green infrastructure?
2. What is the adaptive potential of blue-green infrastructure across 11,041 cities in the European Union?
3. Do cities in different climate zones differ in their current capacity for adaptation using blue-green infrastructure?

2. Materials and Methods

The CCI was developed based on a multi-stage analysis (Fig. 1). In the first stage, 2025 satellite data were obtained from the Sentinel-2 mission under the Copernicus program and from Landsat 8 and 9 missions operated by NASA. A set of raster maps was generated from this data: a Land Cover Map and a Vegetation Vigor Map both derived from Sentinel-2 data, and a Surface Radiation Properties Map and a LST Map derived from Landsat 8 and 9 data. The raster maps were used to calculate spatial indicators for the studied cities. These indicators describe characteristics of the urban environment relevant to their adaptive potential, including the share of vegetation cover, ecological connectivity, biologically active area, surface temperature, etc. (Supplementary material). Their values were later normalized. In the next stage, the spatial indicators were thematically grouped into five key aspects reflecting BGI functioning in cities: vegetation state, thermal conditions, water conditions, surface permeability and vegetation diversity, and calculated as integrated indicators. Finally, the integrated indicators were combined into the CCI, which serves as a measure of urban adaptive potential to climate change in relation to BGI functioning.

2.1. The delineation of urban areas

The analysis covers 27 countries of the EU, for which no single, universally accepted definition of a city exists (Rozenblat et al. 2018). For this reason, an operational definition of a city was adopted and a consistent method for delineating urbanized areas was developed (Fig. 2). For consistency, boundaries were defined using a single methodological approach, as administrative city limits vary significantly between countries and could otherwise bias the results. Further in the manuscript, the terms “city” and “urban area” are used interchangeably.

The delineation of urbanized areas was based on the integration of three main datasets: a point layer of city locations enriched with statistical variables obtained from Eurostat (Eurostat 2026a) and national statistical offices, the boundaries of Local Administrative Units (LAU; Eurostat 2026b), and the Degree of Urbanisation (DEGURBA) classification, which reflects population size, population density and settlement density (Eurostat 2026c). Additionally, a raster population dataset (Eurostat 2021) was used to support the identification of densely populated areas. The aggregation and spatial integration of these data

sources enabled the development of consistent urbanized area boundaries across all analysed countries. Each LAU area had to meet specific demographic and spatial criteria to be categorised as a city: a minimum population of 5,000 inhabitants (according to national statistical offices) and an urbanized area of at least 2 km². The area criterion was not mandatory for cities located within larger metropolitan areas, such as the Paris metropolitan area, which includes cities like Gentilly, Vanves, Saint-Mandé and more. In total, 11,041 cities were identified, with a combined urbanized area of 133,894 km².

2.2. Variables Describing Urban Characteristics

In this study, variables characterizing cities by capturing their diverse geographical and demographic conditions, were derived from multiple sources. The majority of them were obtained from Eurostat (2026a). The selection of datasets was guided by their temporal relevance and spatial consistency, ensuring comparability across cities. Therefore, only harmonized and pan-European datasets were used, avoiding reliance on local or country-specific data sources.

Each city is described by the following variables: The Köppen–Geiger climate classification (Peel et al. 2007) represents the dominant climate type of each city based on long-term temperature and precipitation patterns. The data used in this study correspond to the 1991–2020 climatological period and were obtained from established global climate datasets (Beck et al. 2018).

Population represents the number of inhabitants living within the urban area of each city. It is derived from the Eurostat Census Grid 2021, which provides harmonized population data at a high spatial resolution across Europe (Eurostat 2021). Area [km²] represents the spatial extent of the urban area of each city calculated in accordance with the methodology in subsection 2.1. Mean population density [people/km²] represents the average population density within the urban area of a city. It is calculated as the ratio of total population to the urban area (Eurostat 2021). Average height above sea level [m] represents the mean elevation within the urban area of a city. It is derived from the EU-DEM dataset provided by Eurostat, which offers a consistent digital elevation model across Europe (Eurostat, 2026d). Precipitation [mm/year] represents the mean annual precipitation for the period 2000–2023. The data are provided by NASA and derived using the Integrated Multi-satellite Retrievals for GPM (IMERG) algorithm. This approach integrates observations from the Global Precipitation Measurement (GPM) satellite constellation, enabling the generation of high-resolution and globally consistent precipitation estimates (NASA 2020). Latitude [°] represents the geographic position of a city relative to the equator (Eurostat 2026a).

2.3. Raster maps

In this study, satellite data was employed to generate raster maps in order to obtain consistent, spatial information for all EU cities within a single year. Each raster map is generated following a dedicated methodology.

Land Cover Map integrates several data sources: Google Dynamic World – a daily updated land cover dataset provided by Google (Brown et al. 2022), Sentinel-2 L2A - atmosphere-corrected Sentinel-2

imagery (BoA), Sentinel-2 Cloud Score+ (Pasquarella et al. 2023) - a cloud mask dataset provided by Google. Data products within the period 1 April 2025–30 September 2025 were used. For each analyzed city, a multitemporal mosaic was produced by statistically reducing all available maps within the specified period, with the modal (most frequent) value per pixel retained. The 'Built-Up area' class was subdivided into two more specific classes: 'Urbanized areas', comprising impervious surfaces such as dense building structures and roads and 'Managed green areas', including structured urban greenery such as large green belts and tree-lined avenues. This subdivision was based on the "Greenest Index," defined as the 95th percentile of NDVI values derived from all Sentinel-2 scenes within the study period. Subsequently, the Greenest Index values were subjected to a thresholding procedure using the Otsu method (Otsu 1979). The final land cover map therefore distinguishes nine land cover classes: surface water, forests and dense tree cover, low vegetation, croplands, scattered trees and shrubs, wetlands, bare ground, urbanized areas, managed green areas. This information product was resampled to a 20 m resolution.

Vegetation Vigor Map integrates two data sources: Sentinel-2 L2A – atmosphere-corrected Sentinel-2 imagery (BoA) and Sentinel-2 Cloud Score+ – a cloud mask dataset provided by Google. Data from the period 1 June 2025–31 August 2025 were utilized to ensure coverage of peak growing-season conditions. Each cloud-free Sentinel-2 scene within the defined period was used to compute two spectral indices: Normalized Difference Moisture Index (NDMI) and (NDVI) (Möller and Bartlomiejczak 2020). For each index, the statistical reduction was calculated as the 95th percentile of all available values from the analyzed period. The final vegetation vigor map was then derived as the sum of the two 95th-percentile rasters. Consequently, the resulting pixel values range from − 2 to + 2, where higher values indicate greater vegetation vigor. By incorporating both indices, the indicator accounts for chlorophyll content as well as potential water stress experienced by vegetation.

To derive the Land Surface Temperature (LST) Map, Level-2 data from both Landsat 8 and Landsat 9 were utilized. Thermal band 10 was employed. The analysis was conducted for scenes acquired during the summer months (June–August) 2025. Within this dataset, cloud-contaminated pixels were identified and removed using the QA_PIXEL band. Spectral data were masked in areas where thermal observations indicated temperatures below 5°C. The digital numbers were subsequently converted into degrees Celsius using the radiometric rescaling coefficients. The processed data were aggregated by calculating the mean value, which served as the representative statistical measure.

Surface Radiation Properties Map was derived from Landsat 8 and Landsat 9 Level-2 data, specifically using bands B2, B4, B5, B6, B7, and B10. Cloud-contaminated pixels were masked, and the data were converted to surface reflectance values with solar angle correction. In this raster map, spectral data were also masked in areas where thermal observations indicated temperatures below 5°C, as such values were assumed to represent artifacts introduced by the masking procedure. Subsequently, the following indices were calculated for each individual scene included in the analysis: Normalized Difference Built-up Index (NDBI), NDVI and Albedo. The surface radiation properties map was calculated

as 0.5 × (NDVI − 1) × (1 − Albedo). The aggregation of individual scenes into a single mosaic was performed using the mean value. Water bodies were excluded from this raster map.

2.4. Spatial indicators

Spatial indicators provide a quantitative basis for assessing urban environmental conditions and BGI functionality for the given year. They are derived from raster maps and allow the assessment of the five integrated indicators: vegetation state, thermal conditions, water conditions, surface permeability, and vegetation diversity. At an early stage of the analysis, a wide set of spatial indicators was evaluated, however, most of them were excluded due to high correlation with each other. A total of 14 spatial indicators were chosen to the next stage of calculating integrated indicators (Supplementary material).

2.5. Integrated indicators and COOLCITY Index

All spatial indicators were normalized using the minimal-maximal method. If the data distribution deviated from the normal distribution, the Box-Cox transformation was applied to the spatial indicator. Normalized spatial indicators were aggregated by means of a weighted sum to integrated indicators (Supplementary material). For 387 cities, due to the absence of LST data, the integrated indicator “Thermal conditions” was computed solely on the basis of Surface radiation properties, the only available spatial indicator. The weights were determined based on histogram analysis and Principal Component Analysis (Saisana and Saltelli 2011). Finally, the five integrated indicators were combined to calculate CCI. Before aggregation, the integrated indicators were normalized using the minimal-maximal method, and then their values were averaged to obtain CCI. The integration of spatial indicators into integrated indicators constituted a necessary step to ensure a balanced representation of all five spatial aspects in the final CCI, preventing the overrepresentation of any single group of variables. CCI ranged from 0 to 10, where 0 indicates the lowest potential of adaptation to climate change, understood as the greatest challenge for adaptation using BGI and 10 - the highest potential.

The statistical analyses were conducted in R (R Core Team 2026). First, CCI statistics were computed. To examine the relationship between CCI and selected demographic and environmental variables, a linear regression model was fitted, and standardized beta coefficients were estimated together with corresponding significance levels. In addition, comparative analyses of CCI were performed for cities grouped by country and by climate type. For these group-based comparisons, summary measures such as means, quartiles, and value ranges were calculated to assess spatial and climatic variation in adaptive potential.

3. Results

3.1. Which variables characterising European Union cities are correlated with the state of blue-green infrastructure?

Linear regression revealed significant relationships between CCI and a set of independent variables including demographic and environmental factors. The model explained 60% of the variance in CCI (R^2 = 0.60; Fig. 3).

The strongest predictor of CCI is latitude (β = +0.519, p < 0.001), indicating that cities located at higher latitudes achieve higher index values. Among the remaining factors, mean population density [people/km²] (β = −0.408, p < 0.001) is the dominant variable, with increasing density leading to a significant decline in CCI. A significant effect on CCI is also observed for precipitation [mm/year] (β = +0.208, p < 0.001) and average height above sea level [m] (β = +0.161, p < 0.001). Population (β = +0.041, p < 0.001) and area [km²] (β = −0.025, p < 0.001) exhibit statistically significant effects, although clearly weaker than those of the other variables (Fig. 3).

3.2. What is the adaptive potential of blue-green infrastructure across 11,041 cities in the European Union?

The spatial distribution of adaptive capacity across 11,041 cities in the European Union, measured by CCI, indicates a highly differentiated pattern of values (Fig. 4). The mean CCI value is 5.5. A standard deviation of 1.1 indicates moderate variability between cities, while the quartiles of 4.9 (Q1) and 6.3 (Q3) show that half of all cities fall within this range. Extreme values point to substantial differences in levels of adaptive capacity: the lowest value is 0.7, whereas the highest reaches 8.5, highlighting considerable inequalities in cities' ability to adapt to changing environmental and climatic conditions within the EU.

The histogram of the CCI distribution indicates a concentration of values in the moderate to relatively high range: the most frequent interval is < 5.1;6.0 > with 3,888 cities (35%), followed by < 6.1;7.0 > with 3,412 cities (31%) - together, approximately 66% of the studied cities fall within the < 5.1;7.0 > range (Fig. 5). Intervals below 4 include 949 cities (9%), while high values (≥ 7) occur in 819 cities (7%), indicating the presence of a small yet significant group of cities with very low and very high adaptive capacity using BGI (Fig. 5).

Analysis of CCI by European Union countries reveals pronounced differences in urban adaptive capacity using BGI between states (Fig. 6). National average values range from the lowest in Cyprus (2.1) and Malta (3.8), indicating relatively limited environmental capacity to adapt in cities of these countries, to the highest in Finland (7.2), Latvia (7.0), Estonia (6.7) and Sweden (6.6), where cities exhibit substantially greater adaptive potential thanks to their better environmental and spatial conditions. Most countries, including Austria, Belgium, Germany, the Czech Republic, Ireland, and Poland, show average values in the 6–6.5 range (Fig. 6). Southern European countries, such as Spain, Greece, and Italy, have lower average values (approximately 4.5–5.1), indicating a moderate level of adaptive potential using BGI.

An analysis of blue-green infrastructure, grouped by country and city size (based on its populations), reveals significant variations across European Union countries (Fig. 7). In Western European countries such as France, Spain, Italy, and Portugal, large and very large cities with populations exceeding 100,000 inhabitants exhibit relatively low CCI values, ranging from 3.1 to 5.0, indicating a poorer state of BGI. In

the case of small cities, with fewer than 10,000 inhabitants, these values are noticeably higher, falling within the range of 5.1 to 7.0 CCI. Germany and Austria show less internal spatial variation – alongside small urban areas, there are also large cities reaching values between 4.1 and 7.0. Northern European countries, such as Sweden, Finland, Denmark, and Ireland, are characterized by predominantly higher index values, ranging from 5.1 to 8.0. A similar tendency, although with a smaller number of cities, is observed in Estonia, Latvia, and Lithuania. In the group of Central and Eastern European countries, including Poland, Czechia, Slovakia, Hungary, Romania, and Bulgaria, CCI values are varied and generally range between 4.1 and 7.0, while a relatively large number of units in the medium-sized city class (20,000–100,000 inhabitants) reflects the region's fragmented settlement structure (Fig. 7). Mediterranean countries such as Greece, Slovenia, and Cyprus show strong decrease in CCI values with increasing population size, whereas Malta stands out due to its exceptionally small number of urban areas, characterized by low index values ranging from 3.1 to 4.5.

3.3. Do cities in different climate zones differ in their current capacity for adaptation using blue-green infrastructure?

CCI values show differences between cities located in different climate types. The analysis used the Köppen–Geiger climate classification for the 1991–2020 period enabling comparison of cities under similar temperature and precipitation conditions. The overall variation in CCI values between climate types was analyzed across the entire sample of cities (Table 1.). The highest CCI values were obtained in cities located in a cold, no dry season, cold summer climate zone (49 cities), where the mean index value is 7.2 and the quartiles range from 6.9 to 7.5. High CCI values were also obtained in a cold, no dry season, warm summer climate zone (1,787 cities), with a mean of 6.3, an interquartile range of 5.8–6.8, and extreme values from 4.0 to 8.5. The next category includes cities in a temperate, no dry season, warm summer climate zone (4,521 cities), where the mean CCI value is 5.9 and the interquartile range spans from 5.4 (Q1) to 6.4 (Q3), with minimum and maximum values of 2.4 and 8.2, respectively. Lower CCI values are observed in a temperate, no dry season, hot summer climate zone (1,656 cities), where the mean CCI is 5.2 and the interquartile range is 4.7–5.7. In a temperate, dry summer, hot summer climate zone (1,669 cities), the mean CCI value is 4.8, the quartiles are 4.1 and 5.6, and extreme values range from 0.7 to 8.4.Table 1 .

Table 1
Variation of CoolCity Index (CCI) values in cities across different climate types according to the Köppen–Geiger classification 1991–2020 (Peel et al. 2007).

Köppen–Geiger (1991–2020) climate zones	Number of cities	Average CCI	CCI 1st quartile	CCI 3rd quartile	Minimum value CCI	Maximum value CCI
Temperate, no dry season, warm summer	4 521	5.9	5.4	6.4	2.4	8.2
Cold, no dry season, warm summer	1 787	6.3	5.8	6.8	4.0	8.5
Temperate, dry summer, hot summer	1 669	4.8	4.1	5.6	0.7	8.4
Temperate, no dry season, hot summer	1 656	5.2	4.7	5.7	2.8	7.5
Arid, steppe, cold	692	4.2	3.7	4.9	1.7	7.1
Temperate, dry summer, warm summer	297	5.8	5.2	6.5	2.9	7.8
Cold, no dry season, hot summer	198	5.1	4.6	5.6	3.5	7.6
Arid, steppe, hot	103	3.5	2.6	4.3	1.1	6.1
Arid, desert, hot	57	3.4	2.9	3.8	1.9	5.3
Cold, no dry season, cold summer	49	7.2	6.9	7.5	6.2	8.3
Arid, desert, cold	12	3.0	2.6	3.2	2.6	3.7

Among dry climates, higher CCI values were observed in arid, steppe, cold climate zone (692 cities), with a mean of 4.2. Lower values were recorded in arid, steppe, hot climate zone (103 cities), where the mean index drops to 3.5, and in arid, desert, hot climate zone (57 cities), with a mean of 3.4 (Table 1). The lowest CCI values were found in arid, desert, cold climate (12 cities), where the mean index is 3.0 (Table 1).

4. Discussion

4.1. Interpretation of key variables influencing adaptive potential

The obtained results indicate a strong dependence of BGI status, indicated by CCI, on latitude, population density, and precipitation (Fig. 3), which confirms that the adaptive potential of cities based on BGI is shaped both by climatic conditions and urban structure. A significant positive relationship is observed between latitude and CCI-derived BGI condition (β = +0.519), which dominates over the other variables and indicates that cities located at higher latitudes achieve higher index values. This finding is consistent with the conclusions of Chorianopoulos (2002), who emphasized the key role of climatic factors in shaping urban adaptive capacity, as well as with the studies by Guerreiro et al. (2018), which highlight the limiting role of temperature and water deficit in climate change adaptation in cities of Southern Europe. At the same time, the significant negative effect of population density on CCI-derived BGI condition (β = −0.408; Fig. 3) confirms the importance of urban morphology. Intensive urbanization leads to an increase in impervious surfaces, reduction of green areas, and intensification of the urban heat island effect, which directly lowers adaptive potential. Neder et al. (2021) and Kumar et al. (2024) indicate that the spatial structure of a city, particularly building intensity, constitutes a significant barrier to the implementation of nature-based solutions. The regression model explains 60% of the variance in CCI. The observed relationships suggest that the adaptive potential of cities does not result solely from their geographic location, but is significantly modified by spatial structure, the degree of surface sealing, and the availability of space for BGI solutions. In particular, cities with high building density require more intensive and context-specific NBS to compensate for deficits in water, greenery, and surface cooling (Kumar et al. 2024; Pochodyła et al. 2021).

The spatial analysis of BGI status, indicated by CCI, fits into the broader aspect of the differentiation of the adaptive potential of European cities based on BGI. Goldenberg et al. (2021), studying 660 cities in Europe, demonstrated significant relationships between indicators of local climate regulation by BGI and population density. For the entire European sample, the average model fit was $R^2 = 0.34$, while after moving to country-level analyses it increased, particularly in cities of Western Europe, to an average of $R^2 = 0.66$. This indicates that differences between cities in different countries reflect distinct planning, historical, and socio-economic conditions. The authors also emphasized that cities in Western Europe achieved higher R^2 than cities in Eastern Europe, particularly at lower densities, while at high densities exceeding approximately 5,000 people/km², indicators of urban ecosystem service realization approached very low values. These results correspond with the CCI findings, showing a clear decrease in CCI values with increasing population density (β = −0.408, $p < 0.001$; Fig. 3). This means that not only climatic conditions, but also high density significantly limit the implementation of NBS.

4.2. Spatial heterogeneity and regional patterns

The spatial analysis of BGI condition through CCI reveals a clear differentiation in the adaptive potential of cities. The distribution of CCI-derived BGI values is characterized by a distinct concentration in the range of 5.0–7.0, covering approximately 65% of cities (Fig. 5). Extreme values, however, indicate

significant inequalities. The wide range of BGI conditions reflected by CCI values (0.7–8.5) confirms the existence of substantial disparities, approximately 9% of cities are characterized by values below 4 and 6% above 7, indicating a polarization of adaptive potential (Fig. 4). The highest CCI values were recorded in the countries of Northern and North-Eastern Europe, while the lowest were observed in southern countries, which is consistent with the north–south gradient in environmental conditions and urban adaptive capacity described by Oliveira et al. (2022). Cities in Southern Europe operate under conditions of limited water availability, higher temperatures, and more frequent drought episodes, which reduce the effectiveness of BGI, whereas cities in Northern Europe benefit from more favorable conditions for maintaining vegetation and water retention.

The results of the analysis (Table 1), show how significant a city size is in determining the BGI status. Small towns with up to 10,000 inhabitants have the best BGI status, regardless of the country. This trend is most evident in cities in France, Romania, Bulgaria, Greece, Portugal and Italy (Table 1). Similar patterns have been observed in Southeast Asian cities, where larger cities exhibited lower green space percentages and more fragmented green areas (Richards et al. 2017). Similarly, urban expansion in São Paulo and Mexico City has led to significant losses in green spaces, exacerbating urban heat island effects and increasing surface runoff (de Lima et al. 2023) The situation is different in Spain and Cyprus, where a relatively low level of BGI development is already evident even in the smallest towns. In the cities of northern Europe, the relationship between the BGI status and city size is likewise not clearly identifiable.

The obtained CCI results relate to other integrated indicators, which assess the role of BGI in European cities. A popular indicator is the European Green City Index (Shields et al. 2009), which evaluates, among others, the quality of green spaces, water management, and environmental emissions. High index values are achieved by cities in Northern and Central Europe, such as Copenhagen, Stockholm, and Vienna, which is consistent with high CCI values in countries with cooler and more humid climates (Table 1). In contrast, cities in Southern Europe, such as Athens and Rome, obtain lower scores, which also corresponds to lower CCI values in zones with higher temperatures and limited water availability (Table 1). CCI relies exclusively on objective satellite data that capture environmental outcomes. As a result, cities are more likely to improve their index through real, observable changes. Moreover, the use of consistent remote sensing data ensures cross-city comparability.

Similar relationships are also observed with regard to the HUGSI rating (Husqvarna Urban Green Space Insights 2026), which uses satellite data to assess the availability and quality of green spaces in cities worldwide. High HUGSI values are achieved by cities with a large share of green areas, such as Helsinki and Stockholm, which is consistent with the high CCI values observed for Northern European countries. In contrast, lower scores are obtained by cities with high building intensity and limited greenery, such as Madrid and Lisbon, which also corresponds to lower CCI values (Fig. 6). It should be emphasized, however, that HUGSI focuses primarily on the structure and availability of green spaces, whereas CCI additionally integrates thermal and hydrological aspects as well as surface permeability, allowing for a broader representation of the adaptive potential of cities based on BGI and showing the

interdependencies between different environmental components, treating the urban ecosystem as an integrated whole.

4.3. The condition of blue-green infrastructure in relation to climate zones

A differentiation of BGI status, reflected in CCI, between Köppen-Geiger climate zones is evident, indicating a strong dependence of adaptive potential on thermal and hydrological conditions. The highest values observed in *Cold, no dry season, cold summer* climate zone reaching up to 7.2, confirm that environments with a favorable water balance and moderate temperatures support the development and effective functioning of BGI, whereas values of around 3.0 in *Arid, desert, cold* zone reflect increasing constraints related to water deficit and high temperatures (Table 1). This indicates the contextual nature of BGI functioning, as also emphasized by Tyler et al. (2016), that urban resilience indicators should be interpreted in relation to specific environmental conditions. Significant differences are also visible within temperate climates, where a decrease in mean values from 5.9 in *Temperate, no dry season, warm summer* zone to 4.8 in *Temperate, dry summer, hot summer* zone indicates that even small changes in precipitation and temperature conditions translate into differences in adaptive potential (Table 1). The important role of local factors is also indicated by interquartile ranges. In the *Temperate, no dry season, warm summer* zone, the difference between Q1 (5.4) and Q3 (6.4) shows that even under similar climatic conditions, adaptive potential may be significantly modified by other variables, e.g. urban spatial structure (Table 1). At the same time, analysis in other climate types indicates cases of low variability, which may suggest greater homogeneity of adaptive conditions. An example is the *Cold, no dry season, cold summer* zone, where the difference between Q1 and Q3 is considerably smaller (Q1 = 6.9, Q3 = 7.5), similarly in the *Arid, desert, cold* zone with an interquartile range of Q1 = 2.6 and Q3 = 3.2 (Table 1). This may indicate that under these climatic conditions the role of local factors is relatively weaker, and the adaptive potential of cities is shaped primarily by climatic conditions.

4.4. Contribution to the development of integrated indicators

CCI is based on homogeneous remote sensing data, which enables its calculation for a very large number of cities in a comparable and reproducible manner, unlike many previous adaptive indices based on survey or administrative data, which are more difficult to replicate at an international scale (Feldmeyer et al. 2019). CCI can be treated as a complement to existing tools, focusing more strongly on the actual state of the urban environment from a spatial perspective. The methodological value of the indicator is emphasized by its integrative nature, combining multiple aspects of BGI functioning into a single integrated indicator, which corresponds to the conclusions of Tyler et al. (2016) on the need for a multidimensional assessment of urban resilience. Moreover, the use of remote sensing data increases objectivity and significantly enhances the comparative value of the indicator in an international context covering 11,041 cities in the EU. Such an approach fits into the broader trend of research on integrated

environmental and adaptive indicators, whose aim is to simplify complex information and effectively use it in decision-making processes (Alpenberg et al. 2019).

Pochodyła et al. (2021) emphasize that there is no single universal BGI solution for urban water condition problems, and that BGI effectiveness depends on adapting the solution to local conditions. In turn, Almaaitah et al. (2021) show that there are two main strands of using BGI: runoff reduction and mitigation of the urban heat island effect. However, they are often analyzed separately, without a full assessment of co-occurring ecosystem services. In this context, CCI constitutes an important contribution, as it integrates multiple interrelated aspects of BGI functioning, including vegetation state and diversity, water and thermal conditions, and also surface permeability, while also taking into account the temporal dimension of the data through annual-scale analysis and facilitating their systematic updating in subsequent years.

4.5. Practical applications of the new index

Although the CCI results show that cities in Southern Europe face greater adaptive pressure, thus requiring more effort for successful adaptation based on BGI (Fig. 4), increasing thermal stress and water deficit may limit the effectiveness of NBS. These findings should not be interpreted solely as a deficit of green spaces. It highlights a structural limitation in the current configuration of urban adaptation strategies, which remain insufficiently diversified in the face of intensifying climatic stressors. The results suggest that BGI alone cannot compensate for escalating heat and water constraints. This signals a need for a framework that combines both BGI-based solutions with complementary measures, non-NBS measures. Such measures may include heat-reflective “cool roof” and “cool pavement” technologies, increasing urban albedo through surface material modifications (Lu et al. 2021), as well as architectural and urban design strategies that enhance shading, for example - narrow street canyons (Chatzidimitriou and Yannas 2017) and improve urban ventilation through the planning of airflow corridors (Gu et al. 2020).

An important advantage of CCI is its potential for benchmarking cities. The observed spatial and climatic differentiation indicates that the index can be used to identify groups of cities with similar conditions and adaptive needs, serving as a tool supporting decision-making processes and the exchange of experience between cities facing similar challenges (Figueiredo et al. 2018). In doing so, CCI enables intercity comparison and facilitates the exchange of information on best practices in climate change adaptation among cities with similar climates and spatial structures. CCI can also support the identification of cities with low adaptive potential that require further attention and consideration of possible nature-based interventions. It may serve as a tool to support the implementation and monitoring of BGI effectiveness across the continent, as well as in specific regions (European Commission 2021).

4.6. Limitations of index and future research directions

A limitation of CCI is its foundation in spatial data, which means that it does not fully include the social and financial aspects. As indicated by Figueiredo et al. (2018), urban resilience simultaneously

encompasses economic and social aspects, which means that CCI should not be interpreted as a comprehensive measure of adaptation, but rather as an important component of a system assessing adaptive potential. Additional limitations result from the use of remote sensing, which do not allow for the estimation of NBS smaller than the spatial resolution of the satellite data used. Moreover, the quality of the results is influenced by the accuracy of raster maps derived from satellite data and the level of detail of the adopted classification legend, which may lead to interpretative simplifications in the analysis of land cover differentiation.

In practice, CCI can serve as a connecting tool between environmental analysis and planning, constituting a first stage of diagnosis that should subsequently be complemented by local considerations, including urban policy, technical feasibility, and costs, in line with the approach proposed by Tyler et al. (2016). Consequently, future research should focus on integrating CCI with qualitative analyses and social variables, as well as on introducing a temporal component enabling the monitoring of changes and the assessment of the effectiveness of adaptive measures (Feldmeyer et al. 2019).

The main direction for the development of CCI applications is its potential use in a system for continuous monitoring of changes in the urban environment. Currently available datasets, such as CLMS (Copernicus Land Monitoring Service 2026), are insufficient as they are not produced annually. CCI may be a more flexible tool that can be updated annually and monitor the current state of changes in the urban environment more effectively at the European scale.

In the future, CCI may also be combined with climate scenarios based on CMIP6 (Copernicus Climate Change Service 2022), enabling a shift from assessing the current state to analysing potential changes under different climate development projections. Such an approach would allow the identification of areas particularly vulnerable to the intensification of climate extremes and the assessment of BGI resilience under different scenarios. As a result, CCI could be transformed into a tool supporting adaptive planning, taking into account uncertainty and the range of possible future climate conditions, rather than being limited to diagnosing the current state.

5. Conclusions

The conducted analyses confirm that the CCI is a coherent indicator for assessing the adaptive capacity of cities in the context of climate change, integrating various forms of BGI, like vegetation state and diversity, water and thermal conditions, and also surface permeability. The obtained results indicate clear spatial and climatic variation BGI conditions represented in CCI values across the European Union, with a dominant role of climatic factors like latitude, and precipitation in shaping the adaptive potential of the urban environment. Population density is also significant, as it constrains the implementation of NBS. The results of cross-country and climatic analyses indicate a north–south gradient, in which cities in Northern Europe achieve higher index values than those in the south, reflecting environmental differences. A correlation was also found between the BGI status and city size. In many European

countries (France, Romania, Bulgaria, Greece, Portugal and Italy), cities with larger populations have a lower BGI status.

At the same time, the CCI provides a meaningful methodological contribution through its derivation from remote sensing data, enabling large-scale city comparisons in an objective and replicable way. This indicator can serve as a tool to support decision-making processes, identify areas requiring possible intervention, and benchmark cities with similar environmental and spatial conditions. In the future, it is advisable to further develop the indicator by integrating socio-economic data, incorporating a temporal component, and adapting it to regional specificities, which would enhance its usefulness in planning and monitoring urban adaptation efforts.

Abbreviations

CCI
COOLCITY Index
BGI
Blue-Green Infrastructure
NBS
Nature-Based Solutions
LST
Land Surface Temperature
NDBI
Normalized Difference Built-up Index
NDVI
Normalized Difference Vegetation Index
NDMI
Normalized Difference Moisture Index
EU
European Union

Declarations

Funding

The LIFECOOLCITY project, titled "Use of remote sensing for management of blue-green infrastructure in the process of city adaptation to climate change", is being implemented under the LIFE program: LIFE-2023-SAP-CLIMA-CCA - Climate Change Adaptation, no. 101074553. The project is 95% funded by the LIFE program and the National Fund for Environmental Protection and Water Management, with the remaining 5% contributed by the Consortium. The project activities are planned for the years 2023–2029.

Competing Interests

The authors have no relevant financial or non-financial interests to disclose.

Ethics approval and consent to participate

Not applicable.

Author contributions:

Dominik Kopeć - Supervision, Funding acquisition, Project administration, Conceptualization, Methodology, Investigation, Writing - Review & Editing,

Agata Tarkowska - Conceptualization, Methodology, Validation, Formal analysis, Visualization, Writing - Original Draft, Writing - Review & Editing,

Jan Jedliński - Methodology, Software, Formal analysis, Resources, Writing - Original Draft,

Dominik Żmuda - Methodology, Software, Formal analysis, Resources, Writing - Original Draft,

Martyna Wietecha - Methodology, Formal analysis, Data Curation, Writing - Original Draft,

Łukasz Sławik - Funding acquisition, Project administration,

Aram Takmadżan - Methodology, Software, Formal analysis, Resources, Writing - Original Draft,

Aleksandra Krzywicka - Visualization,

Alicja Śniadach - Writing - Original Draft, Writing - Review & Editing,

Robert Migas - Methodology, Software, Formal analysis,

Zuzanna Kunert - Validation, Writing - Review & Editing,

Jakub Charyton - Methodology, Software

References

1. Almaaitah T, Appleby M, Rosenblat H, Drake J, Joksimovic D (2021) The potential of blue-green infrastructure as a climate change adaptation strategy: a systematic literature review. Blue-Green Syst 3(1):223–248. https://doi.org/10.2166/bgs.2021.016
2. Alpenberg J, Wnuk-Pel T, Adamsson P, Petersson J (2019) The use of environmental performance indicators in the greenest city in Europe. Balt J Manag 14(1):122–140. https://doi.org/10.1108/BJM-01-2018-0028
3. Araya-Muñoz D, Metzger MJ, Stuart N, Wilson AMW, Alvarez L (2016) Assessing urban adaptive capacity to climate change. J Environ Manage 183:314–324. https://doi.org/10.1016/j.jenvman.2016.08.060

4. Balany F, Ng A, Muttil N, Muthukumaran S, Wong M (2020) Green infrastructure as an urban heat island mitigation strategy—a review. Water 12:3577. https://doi.org/10.3390/w12123577
5. Beck HE, Zimmermann NE, McVicar TR, Vergopolan N, Berg A, Wood EF (2018) Present and future Köppen-Geiger climate classification maps at 1-km resolution. Sci Data 5:180214. https://doi.org/10.1038/sdata.2018.214
6. Brown CF, Brumby SP, Guzder-Williams B, Birch T, Hyde SB, Mazzariello J, Czerwinski W, Pasquarella VJ, Haertel R, Ilyushchenko S, Schwehr K, Weisse M, Stolle F, Hanson C, Guinan O, Moore R, Tait AM (2022) Dynamic World, near real-time global 10 m land use land cover mapping. Sci Data 9(1):251. https://doi.org/10.1038/s41597-022-01307-4
7. Chahbi M, El Ganadi Y, Idrissi Gartoumi K, Moujoud L, Himeur Z (2025) Assessment of urban greening in Fez, Morocco: an integrated analysis combining remote sensing data analysis and urban policy review. https://doi.org/10.1007/s43995-025-00188-z. J Umm Al-Qura Univ Eng Archit
8. Chan L, Hillel O, Werner P, Holman N, Coetzee I, Galt R, Elmqvist T (2021) Handbook on the Singapore index on cities' biodiversity (also known as the city biodiversity index). Secretariat of the Convention on Biological Diversity and National Parks Board, Montreal and Singapore
9. Chatzidimitriou A, Yannas S (2017) Street canyon design and improvement potential for urban open spaces; the influence of canyon aspect ratio and orientation on microclimate and outdoor comfort. Sustain Cities Soc 33:85–101. https://doi.org/10.1016/j.scs.2017.05.019
10. Chorianopoulos I (2002) Urban restructuring and governance: north-south differences in Europe and the EU URBAN initiative. Urban Stud 39(4):705–726. https://doi.org/10.1080/00420980220119534
11. Copernicus Climate Change Service (2022) Climate extreme indices and heat stress indicators derived from CMIP6 global climate projections. https://doi.org/10.24381/cds.776e08bd. Accessed 23 Mar 2026
12. Copernicus Land Monitoring Service (2026) Land monitoring service. https://land.copernicus.eu/en. Accessed 23 Mar 2026
13. de Lima GN, Fonseca-Salazar MA, Campo J (2023) Urban growth and loss of green spaces in the metropolitan areas of São Paulo and Mexico City: effects of land-cover changes on climate and water flow regulation. Urban Ecosyst 26(6):1739–1752. https://doi.org/10.1007/s11252-023-01394-0
14. Dematteis G (2019) Introduction. Cities as nodes of urban networks. In: Dematteis G (ed) The Italian urban system. Routledge, London, pp 1–16
15. Deslauriers MR, Asgary A, Nazarnia N, Jaeger JAG (2018) Implementing the connectivity of natural areas in cities as an indicator in the City Biodiversity Index (CBI). Ecol Indic 94:99–113. https://doi.org/10.1016/j.ecolind.2017.02.028
16. Di Cristofaro M, Di Pirro E, Ottaviano M, Marchetti M, Lasserre B, Sallustio L (2022) Greener or greyer? Exploring the trends of sealed and permeable spaces availability in Italian built-up areas during the last three decades. Forests 13(12):1983. https://doi.org/10.3390/f13121983

17. Di Palma M, Rigillo M, Leone MF (2024) Remote sensing technologies for mapping ecosystem services: an analytical approach for urban green infrastructure. Sustainability 16(14):6220. https://doi.org/10.3390/su16146220
18. Dimitrov S, Iliev M, Borisova B, Semerdzhieva L, Petrov S (2024) A methodological framework for high-resolution surface urban heat island mapping: integration of UAS remote sensing, GIS, and the local climate zoning concept. Remote Sens 16(21):4007. https://doi.org/10.3390/rs16214007
19. Dobkowitz S, Bronstert A, Heistermann M (2025) Water retention by green infrastructure to mitigate urban flooding: a meta-analysis. Urban Water J 22(5):477–492. https://doi.org/10.1080/1573062X.2025.2472325
20. European Commission (2019) Commission staff working document: guidance on a strategic framework for further supporting the deployment of EU-level green and blue infrastructure. SWD(2019) 193 final. European Commission, Brussels
21. European Commission (2021) Smart cities and communities. European Commission, Brussels
22. European Environment Agency (2024) Urban adaptation in Europe: what works? Implementing climate action in European cities. EEA Report No 14/2023. Publications Office of the European Union, Luxembourg
23. European Environment Agency (2025) Drought impact on ecosystems in Europe. Publications Office of the European Union, Luxembourg
24. Eurostat (2021) Census grid 2021 – GISCO. European Commission, Brussels. https://ec.europa.eu/eurostat/web/gisco/geodata/population-distribution/population-grids. Accessed 23 Mar 2026
25. Eurostat (2026a) Database – Eurostat regional data. European Commission, Brussels. https://ec.europa.eu/eurostat/data/database. Accessed 23 Mar 2026
26. Eurostat (2026b) Local administrative units (LAU). European Commission, Brussels. https://ec.europa.eu/eurostat/web/nuts/local-administrative-units. Accessed 23 Mar 2026
27. Eurostat (2026c) Degree of urbanisation – GISCO. European Commission, Brussels. https://ec.europa.eu/eurostat/web/gisco/geodata/population-distribution/degree-urbanisation. Accessed 23 Mar 2026
28. Eurostat (2026d) EU-DEM – digital elevation model (aspect). European Commission, Brussels. https://ec.europa.eu/eurostat/web/gisco/geodata/digital-elevation-model/eu-dem. Accessed 23 Mar 2026
29. Falda M, Adamos G, Rađenović T, Laspidou C (2025) Mitigating the urban heat island effect and heatwaves impact in Thessaloniki: a satellite imagery analysis of cooling strategies. Sustainability 17(24):10906. https://doi.org/10.3390/su172410906
30. Farooq B, Manocha A (2024) Satellite-based change detection in multi-objective scenarios: a comprehensive review. Remote Sens Appl Soc Environ 34:101168. https://doi.org/10.1016/j.rsase.2024.101168

31. Feldmeyer D, Wilden D, Kind C, Kaiser T, Goldschmidt R, Diller C, Birkmann J (2019) Indicators for monitoring urban climate change resilience and adaptation. Sustainability 11(10):2931. https://doi.org/10.3390/su11102931
32. Ferreira JC, Dos Santos DC, Campos LC (2024) Blue-green infrastructure in view of integrated urban water management: a novel assessment of an effectiveness index. Water Res 257:121658. https://doi.org/10.1016/j.watres.2024.121658
33. Figueiredo L, Honiden T, Schumann A (2018) Indicators for resilient cities. OECD Regional Development Working Papers 2018/02. https://dx.doi.org/10.1787/6f1f6065-en
34. Goldenberg R, Kalantari Z, Destouni G (2021) Comparative quantification of local climate regulation by green and blue urban areas in cities across Europe. Sci Rep 11(1):23872. https://doi.org/10.1038/s41598-021-03140-y
35. Gu K, Fang Y, Qian Z, Sun Z, Wang A (2020) Spatial planning for urban ventilation corridors by urban climatology. Ecosyst Health Sustain 6(1):1747946. https://doi.org/10.1080/20964129.2020.1747946
36. Guerreiro SB, Dawson RJ, Kilsby C, Lewis E, Ford A (2018) Future heat-waves, droughts and floods in 571 European cities. Environ Res Lett 13(3):034009. https://doi.org/10.1088/1748-9326/aaaad3
37. Husqvarna Urban Green Space Insights https://hugsi.green/. Accessed 23 Mar 2026
38. IPCC (2021) Climate change 2021: the physical science basis. Cambridge University Press, Cambridge
39. IPCC (2022) Climate change 2022: impacts, adaptation and vulnerability. Cambridge University Press, Cambridge
40. Kumar P, Debele S, Khalili S, Halios C, Sahani J, Aghamohammadi N, Andrade MF, Athanassiadou M, Bhui K, Calvillo N, Cao S, Coulon F, Edmondson J, Fletcher D, Dias de Freitas E, Guo H, Hort M, Katti M, Rodding Kjeldsen T, Lehmann S, Maselli Locosselli G, Malham S, Morawska L, Parajuli R, Rogers C, Yao R, Wang F, Wenk J, Jones L (2024) Urban heat mitigation by green and blue infrastructure: drivers, effectiveness, and future needs. Innovation 5(2):100588. https://doi.org/10.1016/j.xinn.2024.100588
41. Lu Y, Rahman MA, Moore NW, Golrokh AJ (2021) Lab-controlled experimental evaluation of heat-reflective coatings by increasing surface albedo for cool pavements in urban areas. Coatings 12(1):7. https://doi.org/10.3390/coatings12010007
42. Mackres E, Shabou S, Wong T (2023) Calculating indicators from global geospatial data sets for benchmarking and tracking change in the urban environment. World Resources Institute, Washington. https://doi.org/10.46830/writn.22.00123v2
43. Martins CFV, Guerra FC, Ferreira ATDS, Gonçalves RD (2025) Application of an orbital remote sensing vegetation index for urban tree cover mapping to support the tree census. Earth 6(3):87. https://doi.org/10.3390/earth6030087
44. Möller M, Bartlomiejczak K (2020) Urbanes Grün und Stadtklima – Analyse von Vegetation in europäischen Großstädten. Stadtforsch Stat 6:172–182

45. Moreno M, Ortiz P, Ortiz R (2023) Analysis of the impact of green urban areas in historic fortified cities using Landsat historical series and normalized difference indices. Sci Rep 13(1):8982. https://doi.org/10.1038/s41598-023-35844-8
46. Nardo M, Saisana M, Saltelli A, Tarantola S, Hoffman A, Giovannini E (2005) Handbook on constructing composite indicators: methodology and user guide. OECD, Paris. https://doi.org/10.1787/533411815016
47. NASA (2020) IMERG: integrated multi-satellitE retrievals for GPM. https://gpm.nasa.gov/data/imerg. Accessed 23 Mar 2026
48. Neder EA, de Araújo Moreira F, Dalla Fontana M, Torres RR, Lapola DM, Vasconcellos MDPC, Bedran-Martins AMB, Junior AP, Lemos MC, Di Giulio GM (2021) Urban adaptation index: assessing cities readiness to deal with climate change. Clim Change 166(1):16. https://doi.org/10.1007/s10584-021-03113-0
49. Nedkov S, Zhiyanski M, Dimitrov S, Borisova B, Popov A, Ihtimanski I, Yaneva R, Nikolov P, Bratanova-Doncheva S (2017) Mapping and assessment of urban ecosystem condition and services using integrated index of spatial structure. One Ecosyst 2:e14499. https://doi.org/10.3897/oneeco.2.e14499
50. Oliveira A, Lopes A, Soares A (2022) Excess heat factor climatology, trends, and exposure across European functional urban areas. Weather Clim Extrem 36:100455. https://doi.org/10.1016/j.wace.2022.100455
51. Otsu N (1979) A threshold selection method from gray-level histograms. Automatica 11:285–296
52. Pasquarella VJ, Brown CF, Czerwinski W, Rucklidge WJ (2023) Comprehensive quality assessment of optical satellite imagery using weakly supervised video learning. In: Proceedings of the IEEE/CVF conference on computer vision and pattern recognition. IEEE, pp 2125–2135
53. Peel MC, Finlayson BL, McMahon TA (2007) Updated world map of the Köppen-Geiger climate classification. Hydrol Earth Syst Sci 11(5):1633–1644. https://doi.org/10.5194/hess-11-1633-2007
54. Pochodyła E, Glińska-Lewczuk K, Jaszczak A (2021) Blue-green infrastructure as a new trend and an effective tool for water management in urban areas. Landsc Online 92. https://doi.org/10.3097/LO.202192
55. Psatha E (2025) From indicators to insights: measuring urban quality of life in medium-sized Greek cities with the DPRD-20 urban indicator system. Eur J Geogr 16(2):298–313. https://doi.org/10.48088/ejg.e.psa.16.2.298.313
56. R Core Team (2026) R: a language and environment for statistical computing. R Foundation for Statistical Computing, Vienna. https://www.r-project.org
57. Richards DR, Passy P, Oh RRY (2017) Impacts of population density and wealth on the quantity and structure of urban green space in tropical Southeast Asia. Landsc Urban Plan 157:553–560. https://doi.org/10.1016/j.landurbplan.2016.09.005
58. Rozenblat C, Pumain D (2018) Metropolization and polycentrism in the European urban system. In: Rozenblat C, Pumain D, Velasquez E (eds) International and transnational perspectives on urban

systems. Springer, Singapore, pp 117–141. https://doi.org/10.1007/978-981-10-7799-9_6

59. Saisana M, Saltelli A (2011) Rankings and ratings: instructions for use. Hague J Rule Law 3:247–268. https://doi.org/10.1017/S1876404511200058
60. Shields K, Langer H, Watson J, Stelzner K European green city index. Assessing the environmental impact of Europe's major cities., Siemens AG (2009) Munich. https://www.siemens.com/entry/cc/features/greencityindex_international/all/en/pdf/report_en.pdf
61. Simpson EH (1949) Measurement of diversity. Nature 163:688. https://doi.org/10.1038/163688a0
62. Sola-Caraballo J, Serrano-Jiménez A, Rivera-Gomez C, Galan-Marin C (2025) Multi-criteria assessment of urban thermal hotspots: a GIS-based remote sensing approach in a Mediterranean climate city. Remote Sens 17(2):231. https://doi.org/10.3390/rs17020231
63. Tyler S, Nugraha E, Nguyen HK, Van Nguyen N, Sari AD, Thinpanga P, Tran TT, Verma SS (2016) Indicators of urban climate resilience: a contextual approach. Environ Sci Policy 66:420–426. https://doi.org/10.1016/j.envsci.2016.08.004
64. Wagner K, Frick A, Stoeckigt B, Gey S, Lehmler S, Scholz N, Loeffler F, Engnath V, Heiland S, Schubert S, Salim M (2023) Monitoring urban areas for climate change adaptation using remotely sensed indicators in the UrbanGreenEye project. EGU General Assembly Conference Abstracts, EGU-15135. https://doi.org/10.5194/egusphere-egu23-15135

Figures

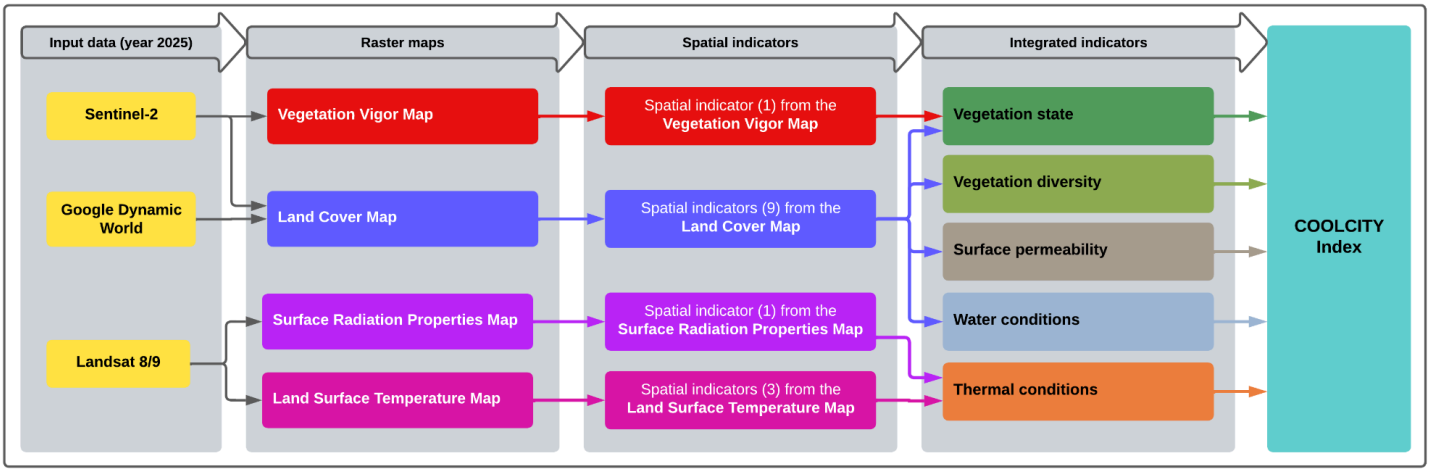


Figure 1

Workflow for the calculation of the COOLCITY Index (CCI).

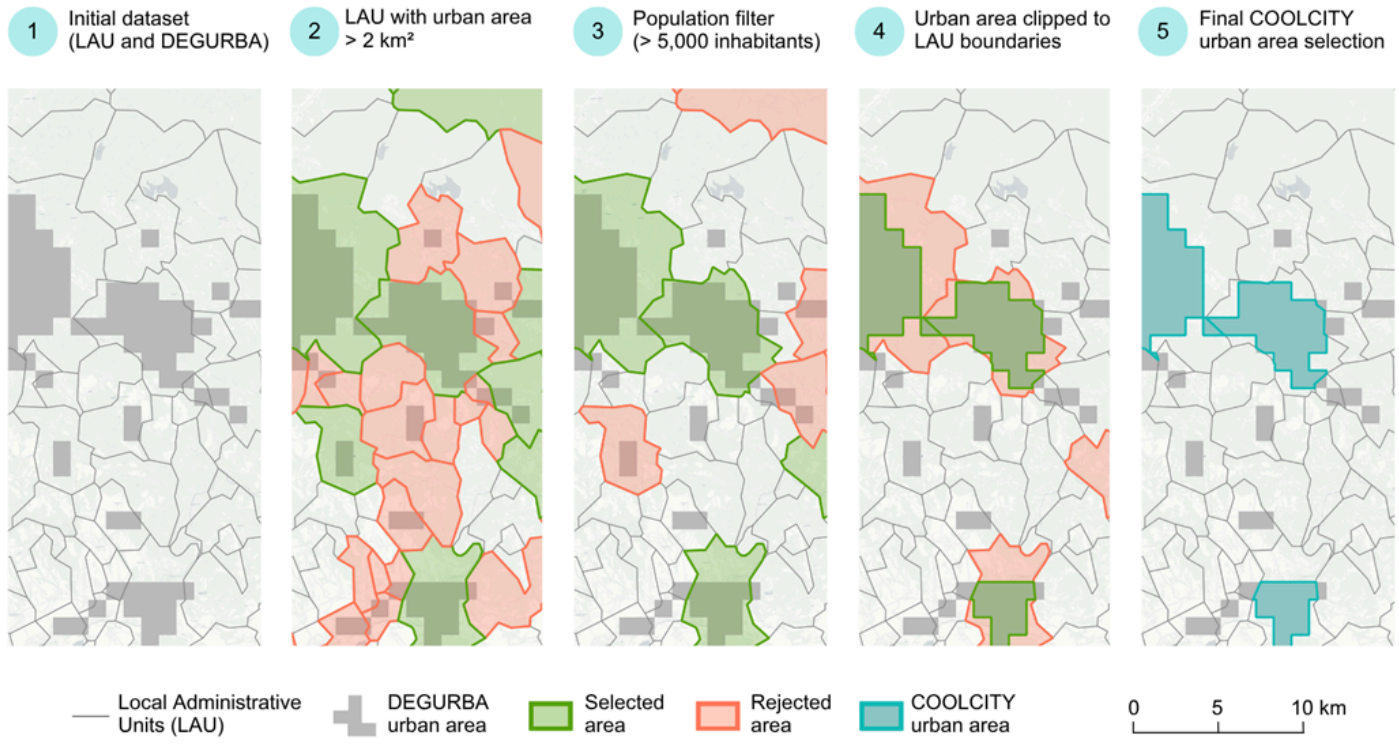


Figure 2

Workflow for the delineation of urbanized areas. LAU - Local Administrative Units, DEGURBA - Degree of Urbanisation.

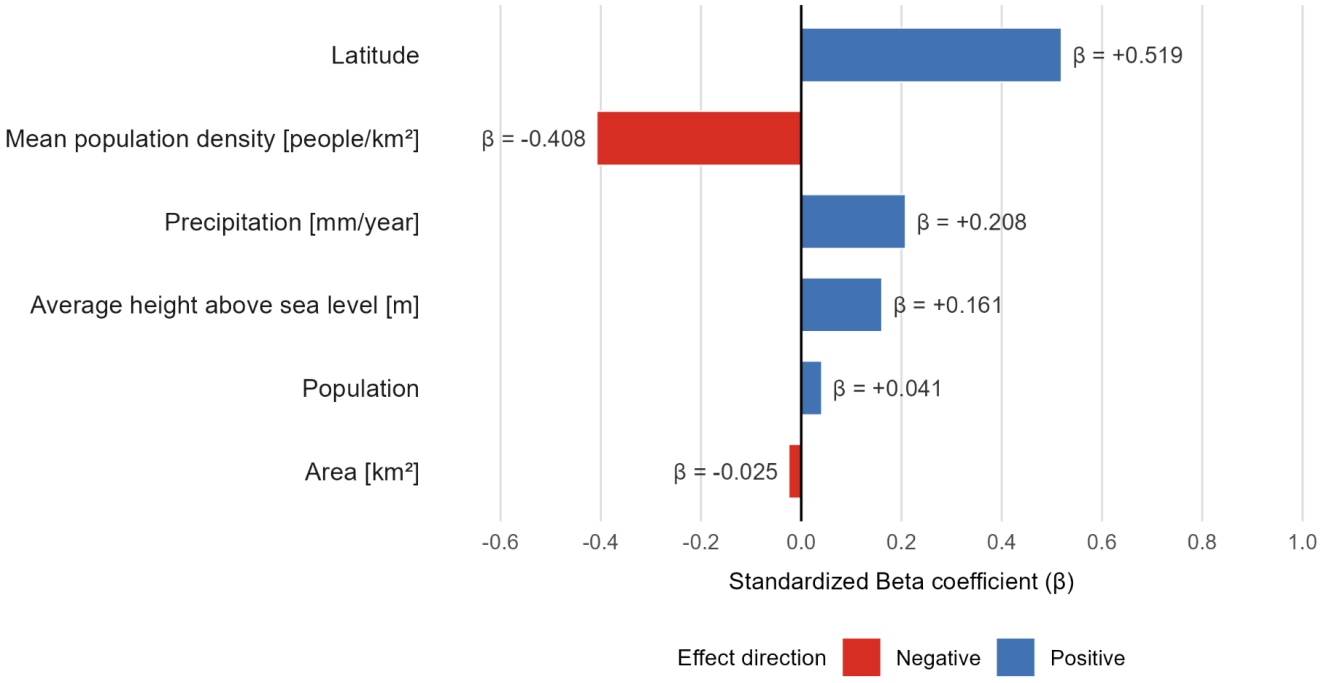


Figure 3

Standardized beta coefficients (β) of the linear regression model.

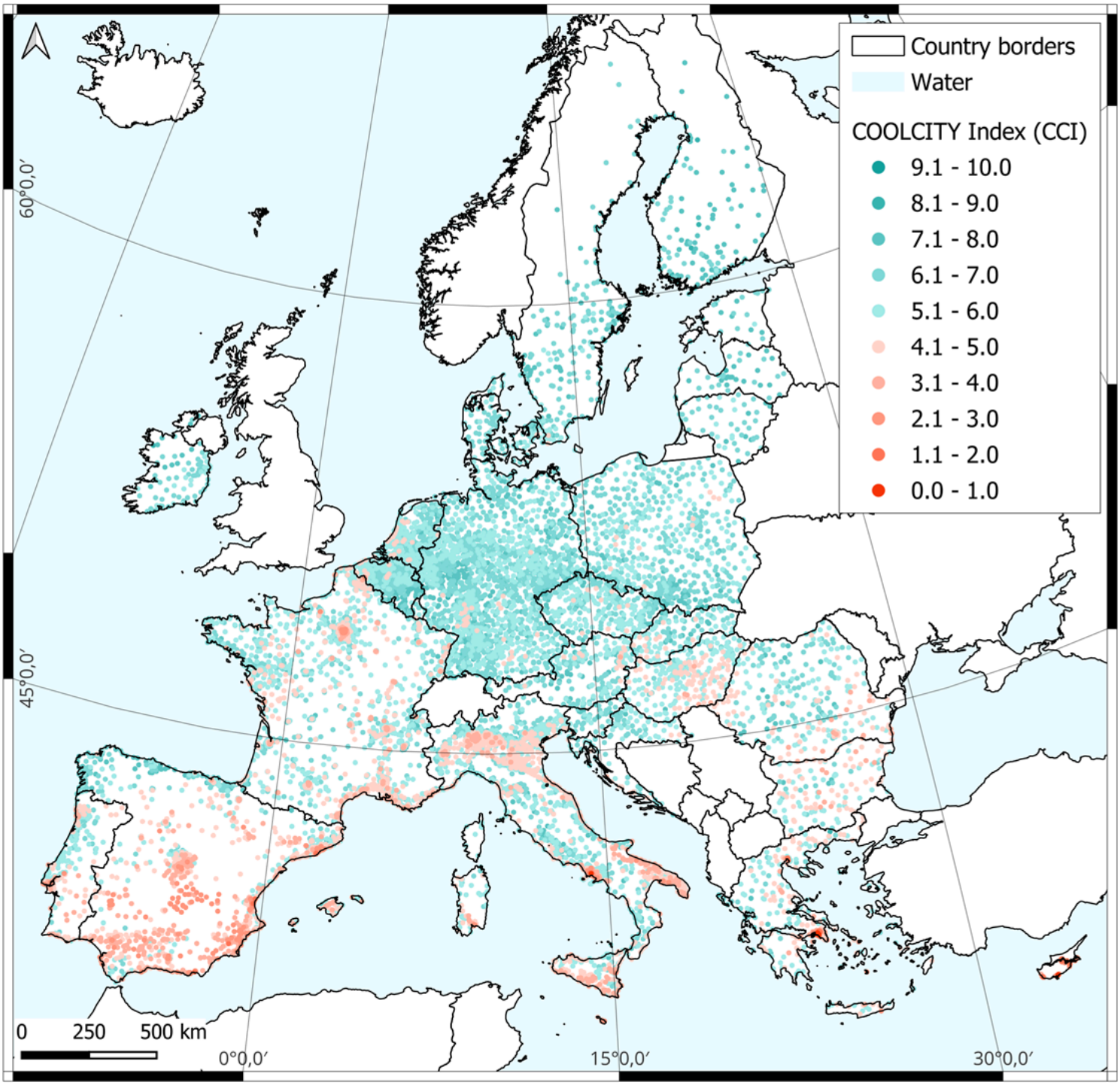


Figure 4

Distribution of COOLCITY Index (CCI) values for 11,041 cities across the European Union.

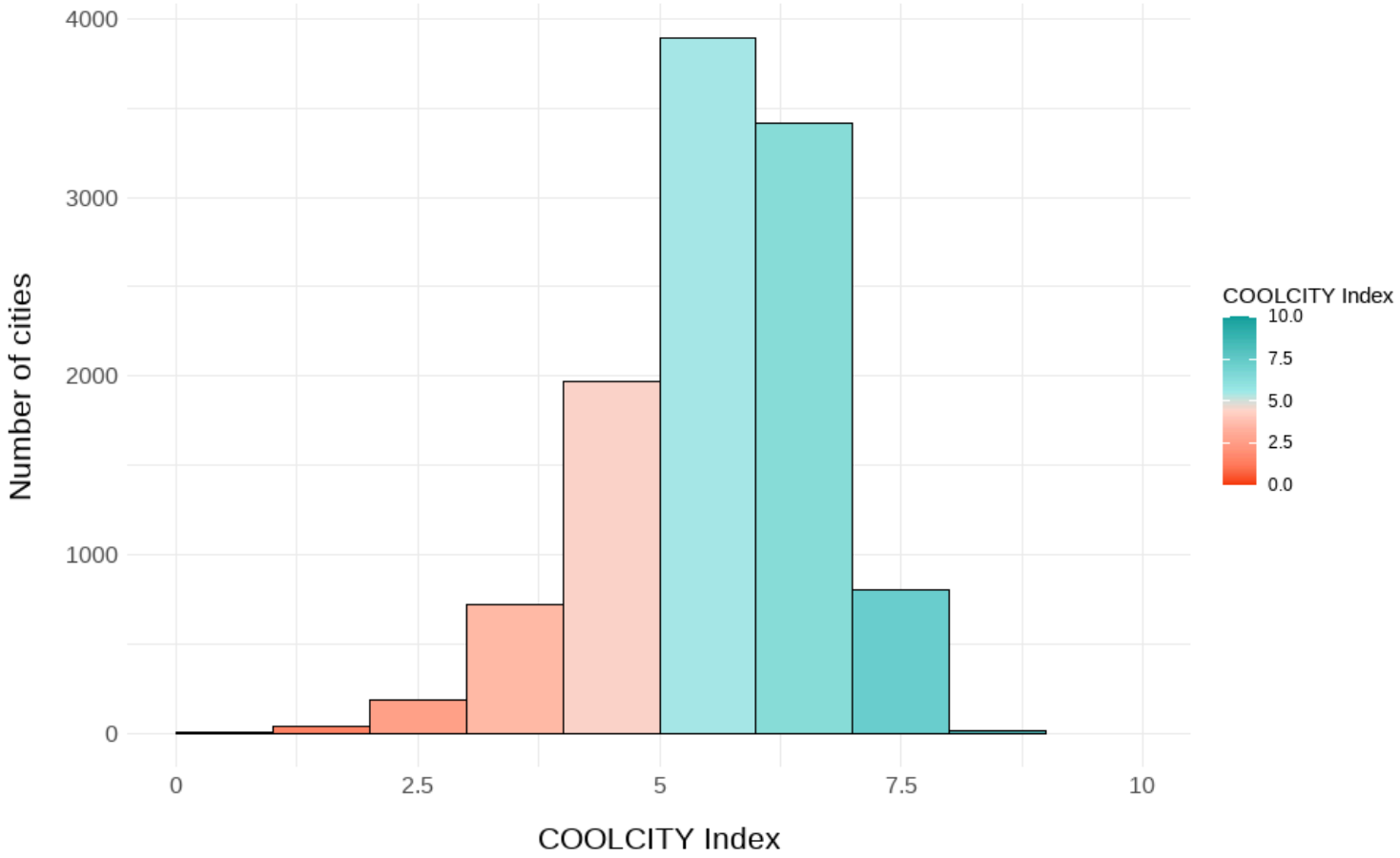


Figure 5

Histogram of the COOLCITY Index (CCI) value distribution.

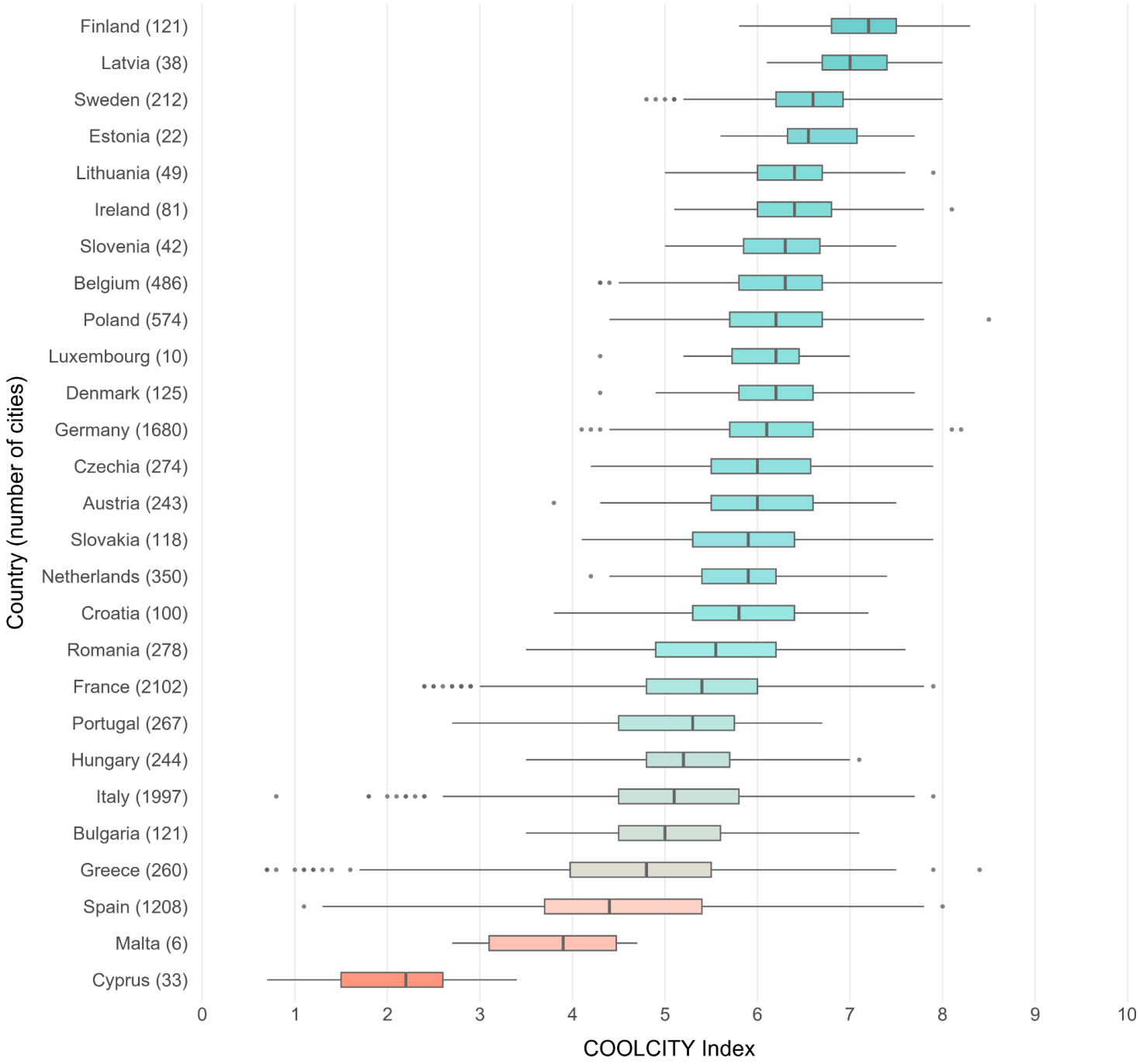


Figure 6

Distribution of COOLCITY Index (CCI) values for cities across European Union countries. The box plot shows the data distribution: the box represents the range of CCI values between the 1st (Q1) and 3rd (Q3) quartiles; the line inside the box represents the mean; the whiskers represent the range of the largest and smallest values not considered outliers; and the points represent outliers. Colors represent different COOLCITY Index (CCI) values, the same as in Figure 4.



Figure 7

Average COOLCITY Index by city size class (population) and EU countries. Circles represent city population classes defined by the number of inhabitants. The axes represent EU countries. Circle size indicates the number of cities in a given size class within each country. Circle color represents the mean COOLCITY Index value for each group.

Supplementary Files

This is a list of supplementary files associated with this preprint. Click to download.

- Supplementarymaterial.docx